Nonlinear forced oscillations of the coupled masses between repelling magnets

Krzysztof Witkowski, Grzegorz Kudra, Sergii Skurativskyi, Grzegorz Wasilewski, Jan Awrejcewicz

Abstract: In these studies, we consider oscillations in the physical model consisting of two carts mounted on a guide. The movement of these carts is restricted by the repelling magnets. The interaction between carts is provided by spring or impact element. The harmonic external loading is applied to one of the carts. To describe this system, the nonlinear mathematical model is developed. The results of model parameter identification are presented. Moreover, the procedure of model validation on the bases of experimental and numerical analysis of system dynamics is discussed as well.

1. Introduction

A large amount of natural and artificial systems incorporates the influences of mechanical, magnetic, and electric fields. When small deviations from the steady state are considered, the description of each field is very similar and can be carried out separately from others. Beyond the linear approach the peculiarities of forces, namely the character of nonlinearity and cooperative effects, are manifested. In particular, a wide range of fascinating phenomena are revealed in the oscillating systems consisting of mechanical elements [1, 2], like a spring, dash-pot or impact, and magnetic parts [3]. Our research is concerned with the studies of cooperative actions of mechanical and magnetic forces, when nonlinear character of both fields is essential. To do this, the magneto-mechanical experimental system performing the forced oscillations is established. Classification of modes observed experimentally, the development of proper mathematical models and their validation keep in our focus as well.

2. Experimental rig

To begin with, let us describe the main steps of experimental studies. Fig. 1 exhibits an experimental stand of two-degree-of-freedom mechanical oscillator with linear mechanical and non-linear magnetic stiffness and external harmonic forcing, modeled and analyzed in the present work.

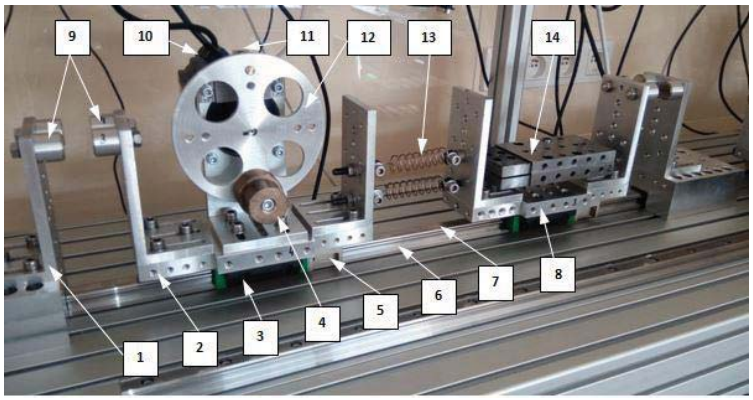

Figure 1. Experimental stand.

The experimental stand consists of two carts (2 and 8) connected with the spring (13) and moving, via linear rolling bearing blocks (3), along a common rail (6). Positions of the carts are measured by the use of Hall sensors (5) and magnetic tape (7) integrated with the bearing blocks and the rail, respectively. The cart (2) is equipped with stepper motor (10) generating harmonic forcing via the disc (12) with an unbalanced mass (4). The transoptor (11) mounted behind the disc (12) allows one to control the absolute angular position of the stepper motor. Both carts on the outer sides have pair of permanent magnets (9) interacting repulsively with the identical ones mounted on the fixed supports (1). Mass of the second cart can be modified by the use of additional mass elements (14).

The peculiarities of experiment procedure can be found in [1]. To be convinced that we correctly understand the observed phenomena, the mathematical model for the experimental stand is developed.

3. Mathematical model

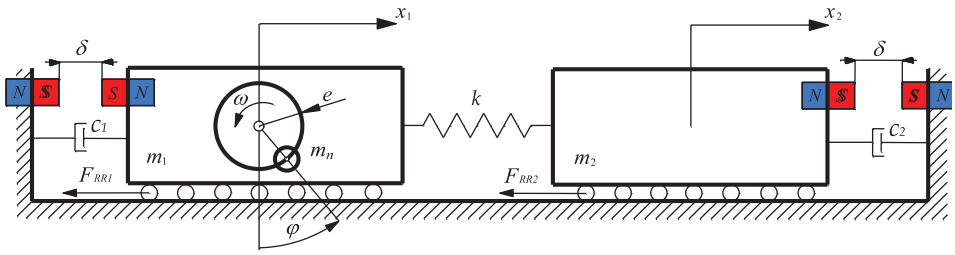

Figure 2. Physical model.

To construct the equations of motion for the experimental rig, let us consider the physical model, presented in Fig.2. The coordinates x_1 and x_2 define the displacements of two masses m_1 and m_2,

connected with the spring of stiffness k. Each mass undergoes the rolling friction force $F_{RRi} = T_i sgn(\dot{x}_i) \approx T_i \frac{\dot{x}_i}{\sqrt{\dot{x}_i^2+\varepsilon_i^2}}$, viscous damping $c_i\dot{x}_i$ and interacts with the wall via the magnetic repulsive force F_M acting between pair of permanent magnets with the gap δ. A disc is mounted on the body of mass m_1 and rotates with the angular frequency of forcing $\dot{\varphi} = \omega$ providing the harmonic external disturbances. An additional unbalanced body of a mass m_n is placed on radius e of the disc. Utilizing the second Newton law leads us to the following equations of motion

$$m_1\ddot{x}_1 + k(x_1 - x_2) + F_{R1}(\dot{x}_1) - F_M(x_1 + \delta) + F_M(\delta) = f_0\dot{\varphi}^2\sin\varphi,$$
$$m_2\ddot{x}_2 + k(x_2 - x_1) + F_{R2}(\dot{x}_2) + F_M(\delta - x_2) - F_M(\delta) = 0, \quad (1)$$

where

$$F_{Ri}(y) = c_i y + T_i \frac{y}{\sqrt{y^2+\varepsilon_i^2}},$$
$$F_M(y) = \frac{F_{M0}}{(d_3y^3+d_2y^2+d_1y+1)^n}.$$

To validate the derived model, at first, we elucidate the degree of magnetic force nonlinearity and establish the analytic expression for it assuming that magnets are the point objects and force magnitude depends only on the distance to the magnet.

4. Parameter's estimation

4.1. Magnetic springs' characteristics

Static characteristics of two (P1 and P2) of four pairs of magnets used in the experimental stand presented in Fig. 1 have been investigated using special equipment. The experimental results along with fit theoretical model in two versions A and B there are presented in Fig. 3, where z is distance between the magnets. The corresponding parameters of the model are given in Tab. 1.

Table 1. Parameters of the magnetic springs' models for pairs of magnets P1 and P2.

Model	Magnets	F_{M0} [N]	n	d_1 [m^{-1}]	d_2 [m^{-2}]	d_3 [m^{-3}]	F_O [mm^2]
A	P1	107.0	3.571	60.37	0	0	0.2401
	P2	101.2	3.771	54.96	0	0	0.1650
	P1, P2	104.4	3.624	58.66	0	0	1.2885
B	P1	109.5	1.727	143.0	186.6	$2.015 \cdot 10^5$	0.0160
	P2	103.1	1.989	115.9	189.1	$1.125 \cdot 10^5$	0.0200
	P1, P2	106.8	1.719	141.1	387.0	$1.919 \cdot 10^5$	1.0916

The objective function F_O is defined as average squared difference between magnetic forces F_M obtained experimentally and from the model.

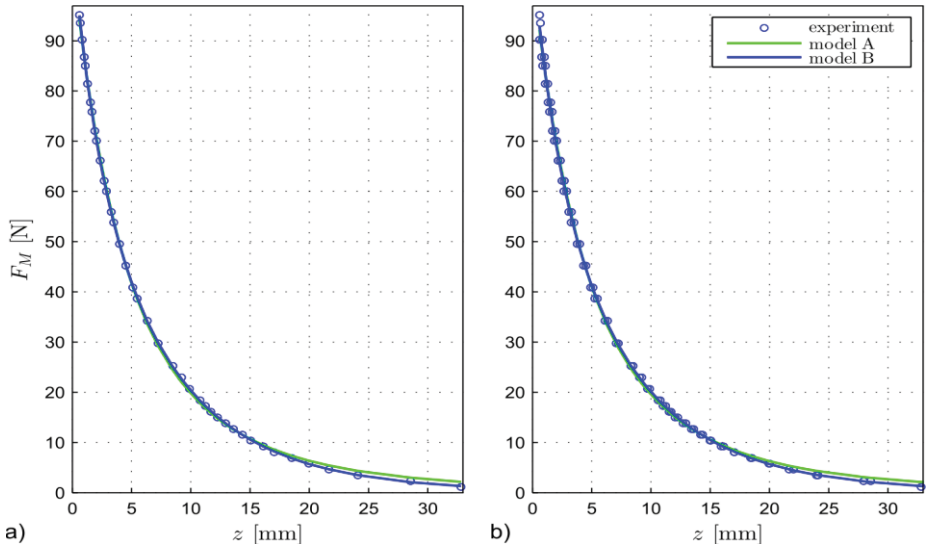

Figure 3. Magnetic springs' characteristics for the pair P1 (a) and the joined data of two pairs of magnets P1 and P2 (b)

4.2. Estimation of the dynamical model parameters

Masses of the carts were measured and assumed to be fixed during identification and all presented numerical simulations: $m_1 = 8.0985$ kg, $m_2 = 6.7838$ kg. Moreover we assume $\varepsilon_1 = \varepsilon_2 = 10^{-6}$ m/s. Additionally the following quantities were measured directly before the experiment used in the identification: $\delta_1 = 0.022984$ m and $\delta_2 = 0.022994$ m, where δ_1 and δ_2 are distances between the magnets on the left and right side of the experimental rig, respectively, when the measurement system is reset. We use ten periodic experimental orbits in the identification process, for the external forcing frequencies: $\omega = 19.37,\ 19.57,\ 19.78,\ 20.995,\ 20.205,\ 20.43,\ 20.62,\ 20.84,\ 21.46,\ 21.665$ rad/s.

The minimized objective function is defined in the following way

$$F_O(\boldsymbol{\mu}) = \frac{1}{2N}\sum_{j=1}^{N}\sum_{i=1}^{2}\frac{w_x\int_{t_{1j}}^{t_{2j}}\left(x_{ije}(t)-x_{ij}(t)\right)^2 dt + w_v\int_{t_{1i}}^{t_{2i}}\left(v_{ije}(t)-v_{ij}(t)\right)^2 dt}{t_{2j}-t_{1j}}, \tag{2}$$

where x_{ij} and v_{ij} are displacement and velocity of ith body in the jth solution obtained numerically from the model, while x_{ije} and v_{ije} are corresponding experimental solutions, $\boldsymbol{\mu}$=(f_0,k,$c_{1,2}$,

$T_{1,2}$,δ,F_{M0}, $d_{1,2,3}$,n) is the set of parameters for estimation. The symbols w_x and w_v stand for the corresponding weights, and they were assumed as $w_x = 0.9\ 1/\text{mm}$ and $w_v = 0.1\ \text{s/mm}$.

The experimental displacements used in the formula (2) are obtained in the following way

$$x_{1je} = x_{1je0} + \delta_1 - \delta,$$

$$x_{2je} = x_{2je0} + \delta - \delta_2, \tag{3}$$

where x_{ije0} is displacement obtained during experiment and burdened with some shift error. Velocities v_{ije} are obtained by numerical differentiation of experimental displacement.

The parameters of magnetic force model were identified again, because of some differences between the four pairs of magnets used in the experimental rig. The estimated values of model parameters obtained after the procedure of minimizing the function $F_O(\boldsymbol{\mu})$ are presented in Table 2.

Table 2. Estimated values of the model parameters.

Model	f_0 [m]	k [N/m]	c_1 [N · s/m]	T_1 [N]	c_2 [N · s/m]	T_2 [N]	δ [m]
A	0.040612	1284.7	4.6298	2.3144	14.408	3.2669	0.022825
B	0.041544	1256.6	2.6617	3.1295	17.164	2.6265	0.022411
Model	F_{M0} [N]	n	d_1 [m^{-1}]	d_2 [m^{-2}]	d_3 [m^{-3}]	F_O	
A	178.40	4.1087	46.946	0	0	2.4345	
B	132.22	1.5283	93.879	201.63	$3.3943 \cdot 10^5$	1.8255	

Using the parameters for model B from Table 2, the solution of system (1) was derived and compared with experimental profile (Fig.4) at different frequencies of external loading ω. We can see the good coincidence of profiles on the intervals of moderate rate of profile growth and permissible its deviation in the vicinity of extrema.

5. Bifurcation dynamics and model validation

Aforementioned results testifying the good agreement between experimental and numerical data at finite time interval and fixed values of parameter ω allow us to continue the model validation and use the Poincaré section technique for the bifurcation diagram construction when the angular frequency $\omega(t)$ increases as shown in Fig.5a. To get the experimental and simulation bifurcation diagrams (Fig.5b-d), the cart positions are sampled at instances fulfilling the condition $\varphi = 2\pi i$, ($i \in Z$). The final part of motion for decreasing forcing frequency was cut off and ignored. It is worth noting that the nonstationarity of $\omega(t)$ does not influence essentially on the bifurcation diagram due to the small rate of ω increasing. Additional comparison of simulation diagrams derived at constant

frequency $\omega(t)$ confirms this conclusion (Fig.5e,f). As shown in Fig.5b, the scenario of period doubling bifurcation is realized at ω increasing. This leads to the chaotic attractor creation.

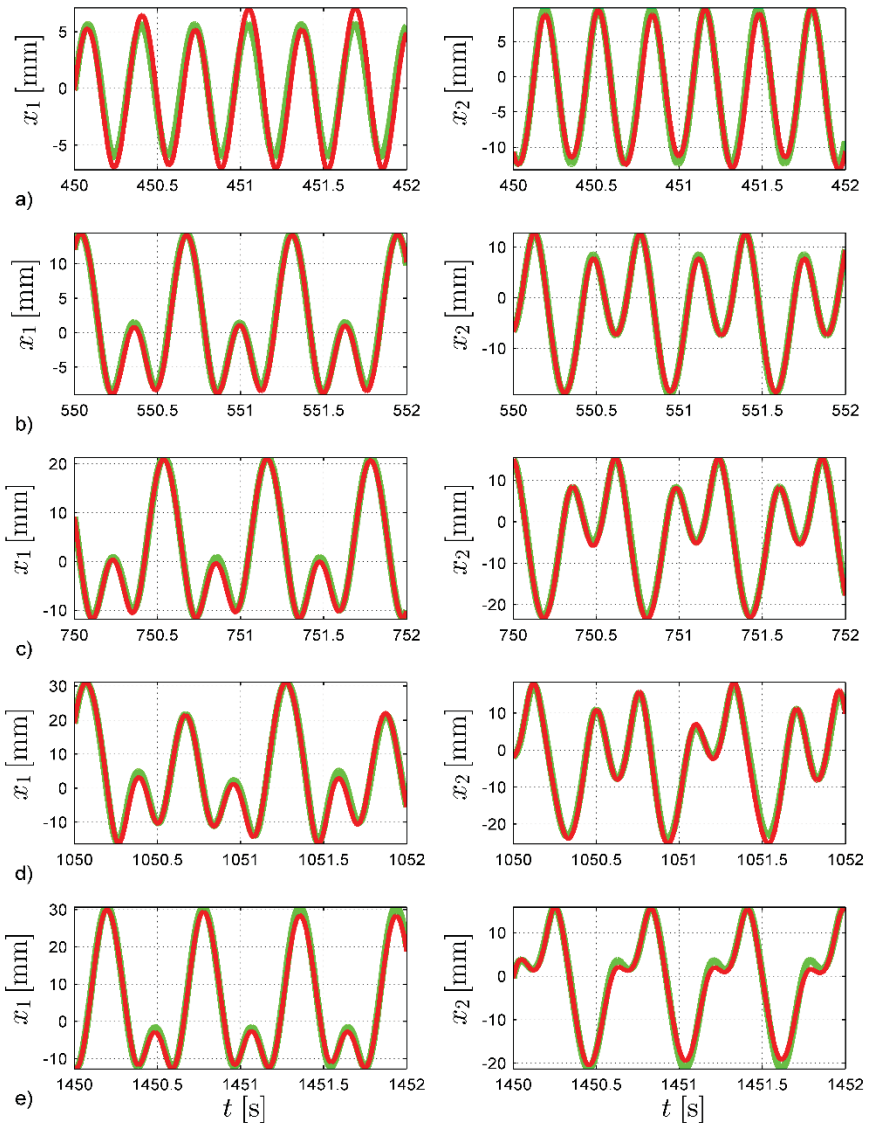

Figure 4. Final agreement between selected periodic experimental solutions (green colour) and the corresponding numerical simulations (red colour) obtained during the model B parameters' estimation, for $\omega = 19.57$ (a), 19.78 (b), 20.205 (c), 20.84 (d), 21.665 rad/s (e).

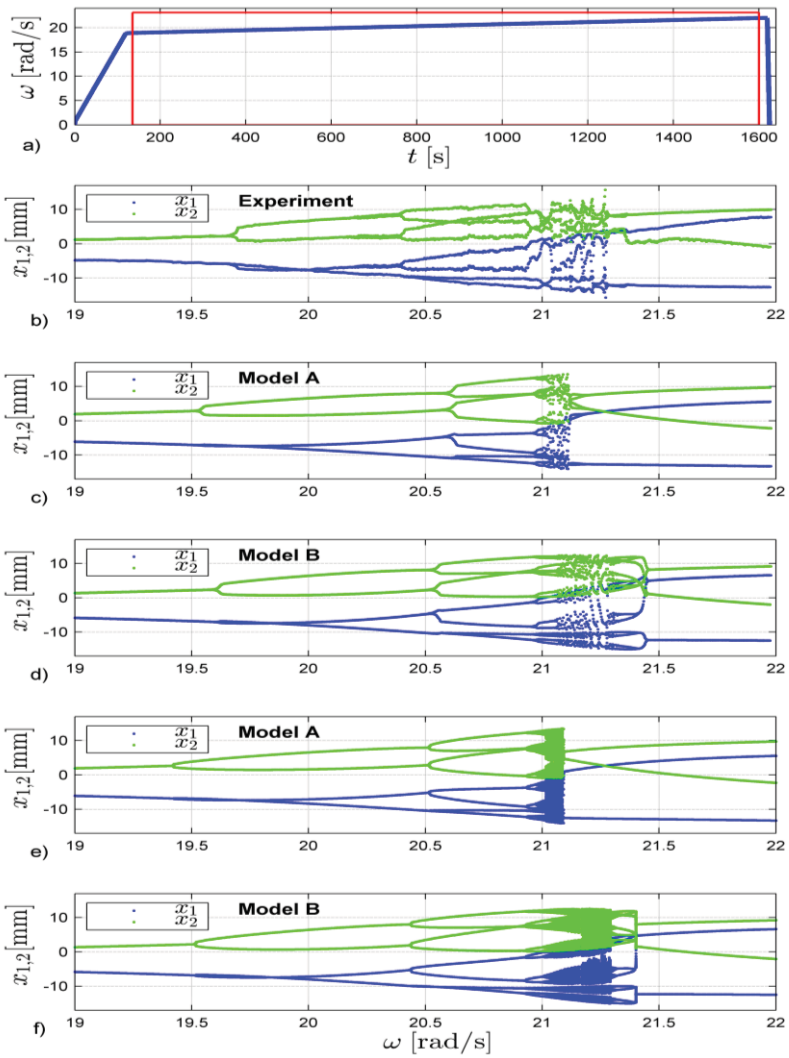

Figure 5. Angular velocity of the forcing $\omega(t)$ applied in the experiment (a) and the corresponding experimental bifurcation diagram (b), bifurcation diagrams of the models A and B obtained for the experimental forcing (c, d) and the corresponding numerical bifurcation diagrams obtained classically (e, f).

There is also the critical value of frequency when an abrupt chaotic attractor collapse is observed. Instead, the stable periodic regime exists. Qualitatively the same behavior demonstrates the model A and B (Fig.5c,d). However, the detailed analysis of bifurcation diagrams shows that the model B matches the experimental data better and, thus, is preferable for the further studies.

6. Conclusions

We thus developed the experimental rig suitable for the studies of mutual influence of mechanical and magnetic forces and validated corresponding mathematical model. We have shown that the magnetic force introduces into the system strong nonlinearity playing the essential role in the formation of complex system's behavior including chaotic. Our results provide the starting point for the detailed analytical and numerical investigations of the developed mathematical model. It should be noted also that the system in question can be easily expanded by incorporating the additional structural elements, for instance impact bond.

Acknowledgments

This work has been supported by the Polish National Science Centre, Poland under the grant OPUS 14 No. 2017/27/B/ST8/01330.

References

[1] Witkowski, K., Kudra, G.,Wasilewski, G., Awrejcewicz, J. Modelling and experimental validation of 1-degree-of-freedom impacting oscillator. *J. Syst. Control Eng.* (2018) 1–13.

[2] Skurativskyi, S., Kudra, G., Wasilewski, G., and Awrejcewicz, J. Properties of impact events in the model of forced impacting oscillator: Experimental and numerical investigations International *Journal of Non-Linear Mechanics* 113 (2019) 55–61.

[3] Wojna, G., Wijata, A., Wasilewski, G., and Awrejcewicz, J. Numerical and experimental study of a double physical pendulum with magnetic interaction *Journal of Sound and Vibration* 430 (2018) 214–230.

Krzysztof Witkowski, M.Sc. (Ph.D. student): Lodz University of Technology/Department of Automation, Biomechanics and Mechatronics, Stefanowskiego 1/15, 90-924, Lodz, Poland (*krzys_wit@wp.pl*). The author gave a presentation of this paper during one of the conference sessions.

Grzegorz Kudra, Associate Professor: Lodz University of Technology/Department of Automation, Biomechanics and Mechatronics, Stefanowskiego 1/15, 90-924, Lodz, Poland (*grzegorz.kudra@p.lodz.pl*).

Sergii Skurativskyi, Associate Professor: Subbotin Institute of Geophysics, Palladin av. 32, Kyiv, Ukraine (*skurserg@gmail.com*).

Grzegorz Wasilewski, PhD: Lodz University of Technology/Department of Automation, Biomechanics and Mechatronics, Stefanowskiego 1/15, 90-924, Lodz, Poland (*grzegorz.wasilewski@p.lodz.pl*).

Jan Awrejcewicz, Professor: Lodz University of Technology/Department of Automation, Biomechanics and Mechatronics, Stefanowskiego 1/15, 90-924, Lodz, Poland (*jan.awrejcewicz@p.lodz.pl*).